7-2010

Analysis of a concentric coplanar capacitive sensor using a spectral domain approach

Tianming Chen
Iowa State University

Jiming Song
Iowa State University, jisong@iastate.edu

John R. Bowler
Iowa State University, jbowler@iastate.edu

Nicola Bowler
Iowa State University, nbowler@iastate.edu

Analysis of a concentric coplanar capacitive sensor using a spectral domain approach

Abstract
Previously, concentric coplanar capacitive sensors have been developed to quantitatively characterize the permittivity or thickness of one layer in multi-layered dielectrics. Electrostatic Green's functions due to a point source at the surface of one- to three-layered test-pieces were first derived in the spectral domain, under the Hankel transform. Green's functions in the spatial domain were then obtained by using the appropriate inverse transform. Utilizing the spatial domain Green's functions, the sensor surface charge density was calculated using the method of moments and the sensor capacitance was calculated from its surface charge. In the current work, the spectral domain Green's functions are used to derive directly the integral equation for the sensor surface charge density in the spectral domain, using Parseval's theorem. Then the integral equation is discretized to form matrix equations using the method of moments. It is shown that the spatial domain approach is more computationally efficient, whereas the Green's function derivation and numerical implementation are easier for the spectral domain approach.

Keywords
capacitive sensors, capacitance measurement, electrodes, electrostatics, integral equations, nondestructive evaluation, QNDE, Electrical and Computer Engineering, Materials Science and Engineering

Disciplines
Electrical and Computer Engineering | Materials Science and Engineering

This article appeared in *AIP Conference Proceedings* 1335 (2011): 1647–1654 and may be found at http://dx.doi.org/10.1063/1.3592126.

ANALYSIS OF A CONCENTRIC COPLANAR CAPACITIVE SENSOR USING A SPECTRAL DOMAIN APPROACH

Tianming Chen, Jiming Song, John R. Bowler, and Nicola Bowler

Citation: AIP Conf. Proc. **1335**, 1647 (2011); doi: 10.1063/1.3592126
View online: http://dx.doi.org/10.1063/1.3592126
View Table of Contents: http://proceedings.aip.org/dbt/dbt.jsp?KEY=APCPCS&Volume=1335&Issue=1
Published by the American Institute of Physics.

ANALYSIS OF A CONCENTRIC COPLANAR CAPACITIVE SENSOR USING A SPECTRAL DOMAIN APPROACH

Tianming Chen[1, 2], Jiming Song[2], John R. Bowler [1, 2], and Nicola Bowler[1, 2, 3]

[1]Center for Nondestructive Evaluation, Iowa State University, Ames, IA 50011
[2]Department of Electrical and Computer Engineering, Iowa State University, Ames, IA 50011
[3]Department of Materials Science and Engineering, Iowa State University, Ames, IA 50011

ABSTRACT. Previously, concentric coplanar capacitive sensors have been developed to quantitatively characterize the permittivity or thickness of one layer in multi-layered dielectrics. Electrostatic Green's functions due to a point source at the surface of one- to three-layered test-pieces were first derived in the spectral domain, under the Hankel transform. Green's functions in the spatial domain were then obtained by using the appropriate inverse transform. Utilizing the spatial domain Green's functions, the sensor surface charge density was calculated using the method of moments and the sensor capacitance was calculated from its surface charge. In the current work, the spectral domain Green's functions are used to derive directly the integral equation for the sensor surface charge density in the spectral domain, using Parseval's theorem. Then the integral equation is discretized to form matrix equations using the method of moments. It is shown that the spatial domain approach is more computationally efficient, whereas the Green's function derivation and numerical implementation are easier for the spectral domain approach.

Keywords: Capacitive Sensor, Multi-Layered Dielectrics, Spectral Domain Approach.
PACS: 41.20.Cv, 02.70.-c, 47.11.Kb, 77.22.Ch.

INTRODUCTION

All The efficient and reliable characterization of material properties of dielectric is of increasing importance in research because of the changing needs of industry. For example, there is greater use of composite materials in new aircraft, such as the Boeing 787, because of the weight saving achieved. Correspondingly, many electromagnetic techniques, both high frequency and low frequency methods, have been developed over the years to meet the increasing need for the nondestructive evaluation (NDE) of dielectric and low-conductivity materials. For instance, dielectric resonators have been developed for precise measurements of complex permittivity and the thermal effects on permittivity for isotropic dielectric materials [1]. Interdigital dielectrometry sensors have been used for applications such as humidity and moisture sensing, electrical insulation properties sensing, monitoring of curing process, chemical sensing, and so on [2]. Cylindrical geometry quasistatic dielectrometry sensors have been developed for quantitative capacitance measurements of multi-layered dielectrics [3], while rectangular coplanar

Review of Progress in Quantitative Nondestructive Evaluation, Volume 30
AIP Conf. Proc. 1335, 1647-1654 (2011); doi: 10.1063/1.3592126

capacitive sensors have been applied for water intrusion detection in composite structures as well as damage detection in laminated composite plates [4].

In our previous work, concentric coplanar capacitive sensors have been developed to characterize quantitatively the permittivity or thickness of each layer in multi-layered dielectrics, using a spatial domain approach in the theoretical analysis [5]. Electrostatic Green's functions due to a point source at the surface of one- to three-layered test-pieces were first derived in the spectral domain, under the Hankel transform. Green's functions in the spatial domain were then obtained by using the appropriate inverse transform. Utilizing the spatial domain Green's functions, the sensor surface charge density was calculated using the method of moments (MoM) and the sensor capacitance was calculated from its surface charge. In the current work, a spectral domain approach is applied. Spectral domain approaches have been widely used in calculating the dispersion characteristics of microstrip lines and open and shielded microstrips over the decades [6]. In this paper, the spectral domain Green's function is used to derive the integral equation for the sensor surface charge density in the spectral domain, using Parseval's theorem. Then the integral equation is discretized to form matrix equations using the MoM. It is shown that the spatial domain approach is more computationally efficient for both one- and three-layered structures in free space, while the Green's function derivation and numerical implementation for the spectral domain approach are more straightforward.

SPECTRAL DOMAIN GREEN'S FUNCTION FOR MULTILAYERED DIELECTRICS

The configuration of the concentric coplanar capacitive sensor is shown in Fig. 1. The capacitive sensor consists of two concentric electrodes: the inner disc and the outer annular ring.

In order to model the in-contact characterization of layered dielectric structures, the Green's function due to a charged sensor over a five-layer half-space dielectric is derived. The Green's function is then utilized in later MoM calculations of the sensor capacitance C. Besides, the test-pieces in our theoretical analysis are assumed to be infinite in the horizontal directions and the sensor electrodes are assumed to be infinitesimally thin.

A charged concentric sensor placed on top of a five-layer half-space dielectric is shown in Fig. 2. The electrostatic potential Ψ, related to the electric field $\mathbf{E} = -\nabla\Psi$, satisfies the Laplace equation in each homogeneous medium, and can be expressed in cylindrical coordinates as

$$\left(\frac{\partial^2}{\partial\rho^2}+\frac{1}{\rho}\frac{\partial}{\partial\rho}+\frac{\partial^2}{\partial z^2}\right)\Psi_i(\rho,z)=0, \qquad i=0,1,\cdots,5, \tag{1}$$

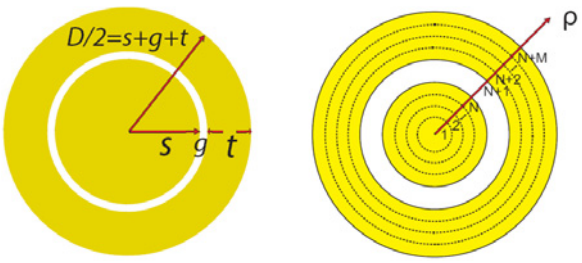

FIGURE 1. Concentric coplanar capacitive sensor. The radius of the central disc and the width of the outer ring are *s* and *t*, and the gap in between is *g*. For computational purposes, the sensor is divided into *N* circular filaments on the inner disc and *M* circular filaments on the outer annular ring.

where $\Psi_i(\rho,z)$ is the potential in medium *i* and is independent of azimuthal angle ϕ. The Hankel transform $\tilde{f}(\kappa)$ of zero-order of a function $f(\rho)$ is given by

$$\tilde{f}(\kappa)=\int_0^\infty f(\rho)J_0(\kappa\rho)\rho d\rho, \tag{2}$$

with the inverse being of the same form. Apply the zero-order Hankel transform (1), making use of the following identity [7]

$$\int_0^\infty\left[\left(\frac{d^2}{d\rho^2}+\frac{1}{\rho}\frac{d}{d\rho}\right)f(\rho)\right]J_0(\kappa\rho)\rho d\rho=-\kappa^2\tilde{f}(\kappa), \tag{3}$$

where $f(\rho)$ is assumed to be such that the terms $\rho J_0(\kappa\rho)df(\rho)/d\rho$ and $\rho f(\rho)dJ_0(\kappa\rho)/d\rho$ vanish at both limits. The spatial domain Laplace equation (1) is then transformed into a one-dimensional Helmholtz equation in the transformed domain:

$$\left(\frac{d^2}{dz^2}-\kappa^2\right)\tilde{\Psi}_i(\kappa,z)=0, \qquad i=0,1,\cdots,5, \tag{4}$$

where for κ the root with positive real part is taken. From (4), general solutions for the potentials in each layer can be expressed as

$$\tilde{\Psi}_i(\kappa,z)=A_i(\kappa)e^{-\kappa z}+B_i(\kappa)e^{\kappa z}, \quad -h_i\le z<-h_{i-1}, \tag{5}$$

where $i=0,1,\cdots,5$, $h_{-1}\to\infty$, $h_0=0$, and $h_5\to-\infty$. Note that $B_0(\kappa)=A_5(\kappa)=0$ due to the fact that the potential at infinity vanishes. The interface conditions on the electric fields are

$$\hat{z}\times\left(\mathbf{E}_0-\mathbf{E}_1\right)=0, \qquad \hat{z}\cdot(\mathbf{D}_0-\mathbf{D}_1)=\sigma_s(\rho) \tag{6}$$

$$\hat{z}\times\left(\mathbf{E}_i-\mathbf{E}_{i+1}\right)=0, \qquad \hat{z}\cdot(\mathbf{D}_i-\mathbf{D}_{i+1})=0 \tag{7}$$

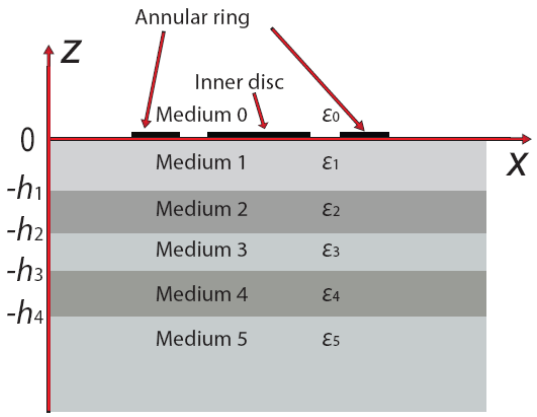

FIGURE 2. Concentric capacitive sensor on top of a five-layer dielectric.

where $i = 1,2,3,4$ and $\sigma_s(\rho)$ is the free surface charge density on the sensor surface and is only a function of ρ. Applying the Hankel transform to the interface conditions for $\mathbf{E}$ and $\mathbf{D}$, the corresponding boundary conditions for the potentials in the spectral domain are expressed:

$$\tilde{\Psi}_0(\kappa,0) = \tilde{\Psi}_1(\kappa,0), \tag{8}$$

$$\epsilon_1 \frac{d\tilde{\Psi}_1(\kappa,0)}{dz} = \epsilon_0 \frac{d\tilde{\Psi}_0(\kappa,0)}{dz} + \tilde{\sigma}_s(\kappa). \tag{9}$$

$$\tilde{\Psi}_i(\kappa,-h_i) = \tilde{\Psi}_{i+1}(\kappa,-h_i), \tag{10}$$

$$\epsilon_i \frac{d\tilde{\Psi}_i(\kappa,-h_i)}{dz} = \epsilon_{i+1} \frac{d\tilde{\Psi}_{i+1}(\kappa,-h_i)}{dz}, \tag{11}$$

where $i = 1,2,3,4$ and $\tilde{\sigma}_s(\kappa)$ is the Hankel transform of the spatial domain surface charge density $\sigma_s(\rho)$ at $z = 0$:

$$\tilde{\sigma}_s(\kappa) = \int_0^\infty \sigma_s(\rho) J_0(\kappa\rho)\rho d\rho. \tag{12}$$

Substitute (5) into (8) to (11) to express the coefficient $A_0(\kappa)$ as

$$A_0(\kappa) = \frac{\tilde{\sigma}_s(\kappa)}{(\epsilon_0+\epsilon_1)\kappa} \frac{F(\kappa)}{D(\kappa)}, \tag{13}$$

$$\begin{aligned} F(\kappa) = {} & 1 - \alpha_2 e^{-2\kappa h_1} - \alpha_3 e^{-2\kappa h_2} - \alpha_4 e^{-2\kappa h_3} - \alpha_5 e^{-2\kappa h_4} + \alpha_2\alpha_3 e^{-2\kappa d_2} + \alpha_3\alpha_4 e^{-2\kappa d_3} + \alpha_4\alpha_5 e^{-2\kappa d_4} \\ & - \alpha_2\alpha_4\alpha_5 e^{-2\kappa(d_1+d_4)} - \alpha_2\alpha_3\alpha_4 e^{-2\kappa(d_1+d_3)} + \alpha_2\alpha_4 e^{-2\kappa(d_2+d_3)} + \alpha_3\alpha_5 e^{-2\kappa(d_3+d_4)} \\ & + \alpha_2\alpha_3\alpha_4\alpha_5 e^{-2\kappa(d_2+d_4)} - \alpha_2\alpha_3\alpha_5 e^{-2\kappa(d_1+d_3+d_4)} - \alpha_3\alpha_4\alpha_5 e^{-2\kappa(d_1+d_2+d_4)} \\ & + \alpha_2\alpha_5 e^{-2\kappa(d_2+d_3+d_4)} \end{aligned} \tag{14}$$

$$\begin{aligned} D(\kappa) = {} & 1 + \alpha_1\alpha_2 e^{-2\kappa h_1} + \alpha_1\alpha_3 e^{-2\kappa h_2} + \alpha_1\alpha_4 e^{-2\kappa h_3} + \alpha_1\alpha_5 e^{-2\kappa h_4} + \alpha_2\alpha_3 e^{-2\kappa d_2} + \alpha_3\alpha_4 e^{-2\kappa d_3} \\ & + \alpha_4\alpha_5 e^{-2\kappa d_4} + \alpha_2\alpha_4 e^{-2\kappa(d_2+d_3)} + \alpha_3\alpha_5 e^{-2\kappa(d_3+d_4)} + \alpha_1\alpha_2\alpha_4\alpha_5 e^{-2\kappa(d_1+d_4)} \\ & + \alpha_1\alpha_2\alpha_3\alpha_4 e^{-2\kappa(d_1+d_3)} + \alpha_2\alpha_3\alpha_4\alpha_5 e^{-2\kappa(d_2+d_4)} + \alpha_2\alpha_5 e^{-2\kappa(d_2+d_3+d_4)} \\ & + \alpha_1\alpha_2\alpha_3\alpha_5 e^{-2\kappa(d_1+d_3+d_4)} + \alpha_1\alpha_3\alpha_4\alpha_5 e^{-2\kappa(d_1+d_2+d_4)} \end{aligned} \tag{15}$$

$\alpha_i = (\epsilon_i - \epsilon_{i-1})/(\epsilon_i + \epsilon_{i-1})$, $i = 1,2,..,5$, and d_1 through d_4 correspond to the thickness of layer 1 to layer 4, respectively. Substitute (13) into (5), the potential in the plane $z = 0$ is expressed as

$$\tilde{\Psi}_0(\kappa,0) = \frac{\tilde{\sigma}_s(\kappa)}{(\epsilon_0+\epsilon_1)\kappa} \frac{F(\kappa)}{D(\kappa)}. \tag{16}$$

Now, rather than performing the inverse Hankel transform of the Green's function in the spatial domain approach [5], the spectral domain Green's function is used to calculate directly the senor surface charge density $\sigma_s(\rho)$ and eventually the sensor capacitance C.

NUMERICAL IMPLEMENTATION

The method of moments (MoM) is utilized in the numerical calculations to calculate the sensor capacitance, C. In the following calculation examples, all the sensors share the configuration shown in Fig. 1, where the central disc is charged to the potential $V_1 = 1$ V and potential of the outer ring is kept at $V_2 = 0$ V.

As shown in Fig. 1, the inner disc (outer annular ring) of the concentric sensor are divided into N (M) circular filaments each with width Δ_1 (Δ_2) and a surface charge density that is constant with respect to variation in ρ. In order to solve for the sensor surface charge distribution $\sigma_s(\rho)$ using MoM calculations, the following expansion for the inner disc is used

$$\sigma_s(\rho) = \sum_{n=1}^{N} \sigma_n b_n(\rho), \tag{17}$$

where σ_n is the unknown coefficient and $b_n(\rho)$ is the pulse basis function:

$$b_n(\rho) = \begin{cases} 1 & (n-1)\Delta_1 < \rho < n\Delta_1 \\ 0 & \text{elsewhere} \end{cases} \tag{18}$$

The Hankel transform of the spatial domain surface charge density $\sigma_s(\rho)$ at $z = 0$ is expressed as

$$\tilde{\sigma}_s(\kappa) = \sum_{n=1}^{N} \sigma_n \tilde{b}_n(\kappa), \tag{19}$$

where

$$\tilde{b}_n(\kappa) = \int_0^\infty b_n(\rho) J_0(\kappa\rho)\rho d\rho = \frac{1}{\kappa}\left[n\Delta_1 J_1(n\Delta_1\kappa) - (n-1)\Delta_1 J_1((n-1)\Delta_1\kappa)\right]. \tag{20}$$

One can expand the surface charge density on the outer annular ring similarly, and (16) is written as

$$\tilde{\Psi}_0(\kappa, 0) = \frac{\sum_{n=1}^{L} \sigma_n \tilde{b}_n(\kappa)}{(\epsilon_0 + \epsilon_1)\kappa} \frac{F(\kappa)}{D(\kappa)}, \tag{21}$$

where $L = M + N$. Multiply both sides of (21) by $\tilde{b}_m(\kappa)\kappa$ and integrate with respect to κ from 0 to ∞, (21) is expressed as the following integral form

$$\frac{1}{\epsilon_0 + \epsilon_1} \int_0^\infty \frac{F(\kappa)}{D(\kappa)} \sum_{n=1}^{L} \sigma_n \tilde{b}_n(\kappa)\tilde{b}_m(\kappa) d\kappa = \int_0^\infty \tilde{\Psi}_0(\kappa, 0)\tilde{b}_m(\kappa)\kappa d\kappa, \tag{22}$$

and can be further discretised into the matrix equation below

$$\begin{pmatrix} G_{11} & G_{12} & \cdots & G_{1L} \\ G_{21} & G_{22} & \cdots & G_{2L} \\ \vdots & \vdots & \ddots & \vdots \\ G_{L1} & G_{L2} & \cdots & G_{LL} \end{pmatrix} \times \begin{pmatrix} \sigma_1 \\ \sigma_2 \\ \vdots \\ \sigma_L \end{pmatrix} = \begin{pmatrix} \tilde{v}_1 \\ \tilde{v}_2 \\ \vdots \\ \tilde{v}_L \end{pmatrix} \tag{23}$$

where

$$G_{mn} = \frac{1}{\epsilon_0 + \epsilon_1} \int_0^\infty \frac{F(\kappa)}{D(\kappa)} \tilde{b}_m(\kappa) \tilde{b}_n(\kappa) d\kappa. \tag{24}$$

On the other hand, from Parseval's theorem, we have

$$\int_0^\infty \tilde{\Psi}(\kappa, z) \tilde{b}_m(\kappa) \kappa d\kappa = \int_0^\infty \Psi(\rho, z) b_m(\rho) \rho d\rho \tag{25}$$

and the right hand side of (23) is expressed as

$$\tilde{v}_m = \int_0^\infty \tilde{\Psi}_0(\kappa, 0) \tilde{b}_m(\kappa) \kappa d\kappa = \int_0^\infty \Psi(\rho, 0) b_m(\rho) \rho d\rho. \tag{26}$$

A closed-form expression can be obtained depending on the constant potential $\Psi_0(\rho, 0)$ on the sensor surface. From (23), the sensor surface charge distribution can be calculated. Once $\sigma_s(\rho)$ is known, one can integrate over the electrode surfaces and find the total charge on both inner and outer electrodes. The sensor output signal, which is the capacitance C between those two electrodes, can be ultimately calculated through

$$C = \frac{Q}{V}, \tag{27}$$

where Q is the total charge on each electrode, while V represents the potential difference between the inner and outer electrodes. It is worth pointing out that there is no singularity problem in evaluating the MoM matrix elements in the spectral domain approach. However, in the spatial domain approach, care must be taken to deal with the singularity problems in the MoM matrix when the source point and the observation point are at the same location.

SPECTRAL VERSUS SPATIAL DOMAIN APPROACHES

The spatial domain Green's function for a source point on top of a four-layer half-space dielectric is derived in [5]. The Green's function is in the form of zero to infinity series summations, and the number of summations is proportional to the number of layers present in the test-piece. In the MoM calculations, the matrix elements are formed by integrating the Green's function along radial and azimuthal directions, where closed form expressions are available for integration along the azimuthal direction. Experimental verification of the numerical model based on the spatial domain Green's function has been

presented in [5]. Very good agreement (to within 4%) between theory and experiment has been observed.

For the purpose of comparing the computational efficiency of the spatial and spectral domain approaches, the case of the concentric sensor on top of a one-layer dielectric slab in free space is considered first. The Green's functions can be obtained by adopting $\epsilon_2 = \epsilon_3 = \epsilon_4 = \epsilon_5 = \epsilon_0$ in Fig. 2. In the following numerical calculations, the zero to infinity summation in evaluating the spatial domain Green's function is truncated to N_0 terms, where N_0 is chosen to achieve accuracy of four significant figures in the final calculated C, and the zero to infinity integral in (24) for the spectral domain approach is truncated to the region from 0 to T in a similar manner. The sensors in the following numerical comparisons share the same configuration: $s = 10$ mm, $g = 0.5$ mm, and $t = 10$ mm. In the numerical calculations, the sensor is divided into $N = M = 10$ circular filaments on the disc and the outer ring, respectively (see Fig. 1). The computer used in the calculations is MacBook Pro with Intel Core 2 Duo 2.26 GHz and 2 GB memory.

Table 1 shows the comparison results for the case of the concentric sensor on top of a one-layer dielectric slab with $\epsilon_{r1} = 100$ in free space. Different slab thicknesses h_1 are considered. As one can see, the spatial domain approach is more efficient in calculating one-layered test-pieces in free space, especially as h_1 increases. Calculations for the dielectric slab with $\epsilon_{r1} = 2$ were also performed. By comparing the calculation results corresponding to $\epsilon_{r1} = 100$ and $\epsilon_{r1} = 2$, it is found that for any fixed h_1, the truncation range and CPU time reduce as ϵ_{r1} decreases, for both approaches. However, such changes are more dramatic for the spatial domain approach. For example, when $\epsilon_{r1} = 2$ and $h_1 = 0.1$ mm, $N_0 = 3$ and the CPU time spent is 7.5 s for the spatial domain approach, while for the spectral domain approach $T = 220$ m^{-1} and the CPU time spent is 55.5 s.

In order to compare the efficiency of these two approaches in calculating C for multi-layered dielectrics, the case of a concentric capacitive sensor on top of a three-layer dielectric test-piece in free space is considered, in which media 0, 2, 4, and 5 in Fig. 2 are replaced by free space while media 1 and 3 share a relative permittivity of ϵ_r. The thickness of layer 1, 2, and 3 is 0.34 mm. Table 2 shows the comparison results between these two approaches, with different permittivity contrasts between neighboring layers. It is still found that the spatial domain approach is more computationally effective than the

TABLE 1. Sensor on top of a one-layer dielectric slab in free space. The relative permittivity of the slab is $\epsilon_{r1} = 100$.

h_1 (mm)	C (pF)	N_0 in the spatial domain approach	Spatial domain approach CPU time (s)	T in the spectral domain approach (m^{-1})	Spectral domain approach CPU time (s)
0.1	6.612	107	72.4	310	79.6
0.56	25.01	49	34.0	490	155.9
3.16	55.10	15	20.3	360	106.6
17.8	71.36	4	8.5	480	204.7
100	71.70	1	5.2	310	154.8

TABLE 2. Sensor on top of a three-layer dielectric in free space, with different permittivity contrasts between neighboring layers. When $\epsilon_r = 40$, four significant figure accuracy in *C* is not achieved.

ϵ_r	*C* (pF)	N_0 in the spatial domain approach	Spatial domain approach CPU time (s)	*T* in the spectral domain approach (m^{-1})	Spectral domain approach CPU time (s)
2	1.688	2	9.0	220	72.5
10	3.370	12	40.4	320	99.9
20	5.288	20	72.7	360	116.8
30	7.140	24	91.4	380	127.6

spectral domain approach, in dealing with multi-layered structures.

CONCLUSION

The computational efficiency of a spectral domain approach is compared with that of a spatial domain approach for the numerical calculation of capacitance of a coplanar concentric sensor in contact with layered test-pieces. The spatial domain approach is found more efficient in dealing with both one- and three-layered dielectric structures, due to the fact that integration of the Green's function along the azimuthal direction has a closed form expression. Such efficiency is at the cost of performing analytical inverse Hankel transformation in the Green's function derivation and at the cost of dealing with singularities in evaluating MoM matrix elements. The spectral domain approach, however, is less complex in both the theoretical derivation and the numerical implementation.

ACKNOWLEDGEMENTS

This material is based upon work supported by the Air Force Research Laboratory under contract FA8650-04-C-5228 and by NASA under cooperative agreement NNX07AU54A at Iowa State University's Center for NDE. Tianming Chen is supported in part by an American Society for Nondestructive Testing graduate fellowship.

REFERENCES

1. J. Krupka, K. Derzakowski, B. Riddle, and J. Baker-Jarvis, *Meas. Sci. Technol*. **9**, pp. 1751--1756 (1998).
2. A. V. Mamishev, K. Sundara-Rajan, F. Yang, Y. Du, and M. Zahn, *Proc. IEEE* **92**, pp. 808--845 (2004).
3. I. C. Shay, and M. Zahn, *IEEE Trans. Dielectr. Electr. Insul.* **12**, pp. 41--49 (2005).
4. A. A. Nassr, and W. W. EI-Dakhakhni, *Smart Mater. Struct.* **18**, 8055014(8pp) (2009).
5. T. Chen, and N. Bowler, *IEEE Trans. Dielectr. Electr. Insul.* **17**, pp. 1307--1318 (2010).
6. Z. Y. Zeng, J. M. Song, and L. Zhang, *IEEE Antennas Wireless Propagation Lett.***6**, pp. 560--563 (2007).
7. C. J. Tranter, *Integral Transforms in Mathematical Physics*, Chapman and Hall, London, 1974.